Nat. Hazards Earth Syst. Sci. Discuss., doi:10.5194/nhess-2016-100, 2016
Manuscript under review for journal Nat. Hazards Earth Syst. Sci.
Published: 4 April 2016
© Author(s) 2016. CC-BY 3.0 License.

Natural Hazards and Earth System Sciences
Discussions

Climate anomalies associated to the occurrence of rockfalls at high-elevation in the Italian Alps

Roberta Paranunzio[1], Francesco Laio[1], Marta Chiarle[2], Guido Nigrelli[2], Fausto Guzzetti[2]

[1]Department of Environment, Land and Infrastructure Engineering, Politecnico di Torino, Italy
[2]Research Institute for Geo-hydrological Protection, National Research Council (CNR IRPI), Italy

Correspondence to: Roberta Paranunzio (roberta.paranunzio@polito.it)

Abstract. Climate change is seriously affecting the cryosphere, in terms, for example of permafrost thaw, alteration of rain/snow ratio, glacier shrinkage. There is concern about the increasing number of rockfalls at high elevation in the last decades. Nevertheless, the impact of climate variables on slope instability at high elevation has not been fully explored yet. In this paper, we investigate 41 rockfalls occurred at high elevation in the Italian Alps between 1997 and 2013 in the absence of an evident trigger. We apply and improve an existing data-based, statistical approach to detect the anomalies of climate parameters (temperature and precipitation) associated to rockfall occurrences. The identified climate anomalies have been related to the spatio-temporal distribution of the events. Rockfalls occurred in association with temperature anomalies in 83 % of our case studies. Temperature represents a key factor contributing to slope failure occurrence in different ways. As expected, warmer temperatures accelerate snowmelt and permafrost thaw; however, surprisingly, negative anomalies are also often associated to slope failures. Interestingly, different regional patterns emerge from the data: higher-than-average temperatures are often associated to rockfalls in the Western Alps, while in the Eastern Alps slope failures are mainly associated to colder-than-average temperatures. The results of this study represent a first step towards the identification of the possible role of climate change in the triggering of slope failures in a mountain environment.

1 Introduction

The recent decades have seen a pronounced warming in global climate, primarily at high elevations and high latitudes (Schär et al., 2004). Air temperature in the European Alps has increased at a rate more than double the global average, and further increases are expected according to global and regional climate models (Beniston, 2006; Stocker et al., 2013). At the same time, an increasing trend of precipitation was observed in the northern hemisphere, with significant regional variations (Auer et al., 2007). Almost everywhere, the cryosphere is degrading rapidly in response to air temperature warming (Nigrelli et al., 2015), and both permafrost thaw and glacier shrinkage worsen mechanical properties of rock, debris and soils, leading to an increase of natural instability (Harris et al., 2009).

Cryosphere degradation might be responsible for the growing number of slope failures at high elevation, in particular rockfalls, that has been documented since the beginning of the 21st century (Chiarle and Mortara, 2008; Stocker et al., 2013). However, the exact role of climate parameters and of their change in

Nat. Hazards Earth Syst. Sci. Discuss., doi:10.5194/nhess-2016-100, 2016
Manuscript under review for journal Nat. Hazards Earth Syst. Sci.
Published: 4 April 2016
© Author(s) 2016. CC-BY 3.0 License.

Natural Hazards and Earth System Sciences
Discussions

the preparation and initiation of slope failure remains poorly understood. Studies on landslide triggering mostly focus on rainfall thresholds (Guzzetti et al., 2008; Brunetti et al., 2015). Only recently, following the summer 2003 heat wave in Europe, the role of temperature in the occurrence of slope failures has been considered thoughtfully (Gruber et al., 2004; Huggel et al., 2010; Stoffel et al., 2014). Authors have speculated on possible relationships between changes of the mean air temperature and an increased activity of slope failures (Ravanel and Deline, 2011) or have explored links between extreme air temperature events and rockfall occurrence (Allen and Huggel, 2013). Paranunzio et al. (2015) proposed a method to investigate the possible role of different climate variables in triggering slope failures, and tested their method on different types of slope instabilities occurred in the Western Italian Alps. This method proved to be able to discriminate slope failures caused by climate factors, and to point out the climate anomaly(ies) that can be deemed responsible for their occurrence.

In this paper, we use an advanced version of the method proposed by Paranunzio et al. (2015) to analyze a catalogue of 41 rock-slope failures occurred from 1997 to 2013 at high elevation in the Italian Alps in the absence of an evident rainfall, seismic or anthropic triggers. The aim is to verify the hypothesis that climate warming can be deemed responsible for increased slope instability in recent years. Our catalogue includes rockfalls and rock avalanches, with volume in the range 10^2-10^6 m^3 (hereinafter, "rockfall" is used to refer to both rockfalls and rock avalanches). Our purpose is to provide a statistical based analysis of the main climate variables in the period preceding the rockfalls, aimed to detect anomalous values that can be deemed responsible for slope failure. We focus first on daily climate variables, including air temperature, the variation in the air temperature, and precipitation (liquid and solid). We then perform a bivariate analysis that includes the climate anomalies identified in the previous step and the spatio-temporal characteristics of the rockfalls in the catalogue (including elevation, aspect, volume, and season of occurrence). Finally, we discuss the results in a context of climate warming, speculating on the possible causes of rockfall occurrence.

2 Study area

We focus on the Italian side of the European Alps. The Italian Alps extend for about 1200 km and cover 5200 km^2, 27.3 % of the European Alps. According to the Alpine Permafrost Index Map, that shows a qualitative index describing how likely is permafrost to exist in the European Alps (Boeckli et al., 2012), many of the rockfalls considered in this work occurred in areas of possible/probable permafrost occurrence. From studies carried out in the European Alps, permafrost on shaded slopes is present above 2500 m, whereas on S-facing slopes it is found above 3500 m (Fischer et al., 2012; Gruber et al., 2004). Climate in the European Alps depends on the complex interaction between orography and the general circulation of the atmosphere (Beniston, 2006). As a result, the Italian Alps show a high variability in the spatial distribution of temperature and precipitation, at regional and local scales (Auer et al., 2007; Brunetti et al., 2009). Referring to the regional scale, the climate regimes of the Western and Eastern Italian Alps differ significantly.

Nat. Hazards Earth Syst. Sci. Discuss., doi:10.5194/nhess-2016-100, 2016
Manuscript under review for journal Nat. Hazards Earth Syst. Sci.
Published: 4 April 2016
© Author(s) 2016. CC-BY 3.0 License.

Natural Hazards and Earth System Sciences
Discussions

In relation to the 30-Year Climate Normals (1981-2010), the total annual precipitation that occurs in mountain areas of the Western and Eastern Italian Alps is about 850 and 1050 mm, respectively. Minimum (maximum) annual temperature is respectively -3 °C (5 °C) in the Western and -1 °C (8 °C) in the Eastern Italian Alps (Esposito et al., 2014).

3 Data

3.1 Rockfall catalogue

Our catalogue lists 41 rockfalls occurred in the 17-year period between 1997 and 2013 at high elevation (above 1500 m) in the Italian Alps (Table 1). The 41 rockfall events concentrate in two main geographical clusters. A first cluster corresponds to rockfalls occurred in the Western Italian Alps; a second cluster includes the rockfalls occurred in the Eastern Italian Alps. Only one case (the Thurwieser rockfall of 18 September 2004) is located in the Central Italian Alps (Fig. 1). More specifically, the rockfalls concentrate in four mountain areas, including (i) the Mont Blanc Massif, (ii) the Matterhorn Peak, (iii) the Monte Rosa Massif, and (iv) the Dolomites. Inspection of Table 1 reveals a cluster of nine rockfall events in 2004. According to local newspapers, 2004 was indeed a crucial year for the high number of rockfalls in the Dolomites and, in general, in the Eastern Italian Alps.

We constructed the catalogue consulting different sources, including national and local newspapers, journal articles, technical reports, and CNR IRPI archives (Fig. 2). For most of the events (25) information on the slope failures was obtained in the framework of a national project aimed to collect information on slope failures in the period from 2000 and 2013 (Brunetti et al., 2015). All the events were located geographically using Google Earth. To select the events listed in the catalogue, we considered the availability of accurate information on the location and the time of occurrence of the failure, and the availability of a long-term record of climate data covering the date of the event. Information on the size of the event is available for 26 rockfalls (63 %), which range in volume between 10^2 and $2x10^6$ m^3 (Table 1).

3.2 Climate data

We considered climate data obtained from 87 meteorological stations pertaining to different networks in the Italian Alps, including networks managed by the Regional Environmental Protection Agencies (ARPA) in Piemonte, Lombardia and Veneto regions, the Centro Funzionale of the Regione Autonoma Valle d'Aosta, the Hydrographic Office of the Provincia Autonoma di Bolzano, and Meteotrentino, in the Provincia Autonoma di Trento. We used different types of climate data, including (i) mean, minimum, and maximum daily air temperature, and (ii) daily cumulated precipitation. In the Italian Alps, meteorological stations located above 1500 m are rare, and many of them were installed only recently. Therefore, climate records in high-mountain areas are limited and have a short duration in the study area. The limited geographical and temporal distribution of the climate information is the main constraint for the analysis of the climate conditions associated to the occurrence of slope failures at high elevation in the Italian Alps. For this reason, the first requirement for the selection of the meteorological stations for our

Nat. Hazards Earth Syst. Sci. Discuss., doi:10.5194/nhess-2016-100, 2016
Manuscript under review for journal Nat. Hazards Earth Syst. Sci.
Published: 4 April 2016
© Author(s) 2016. CC-BY 3.0 License.

Natural Hazards and Earth System Sciences
Discussions

analyses was the availability of a climate record covering the date of the failure and 90 days before it. We then considered only meteorological stations with a climate record exceeding 10 years, and we sought a compromise between the difference in elevation and the planimetric distance between the meteorological stations and the detachment areas. In the end, we used climate data from a total of 27 meteorological stations (Table 2); we checked the quality of all the climate data, to identify and remove possible erroneous values (WMO, 2011).

4 Method

For our work, we exploited the method proposed by Paranunzio et al. (2015), which consists in a bottom-up statistical method for the identification of possible anomalous values of one or more climate variables (V) on the occasion of slope instability events. The idea behind the method is to compare the climate conditions in the period preceding the failure, to the climate conditions typical for the area where the failure has occurred. Eventual outliers of the climate variables prior to the occurrence of a slope failure may be considered related to (and possibly responsible for) the preparation and/or the initiation of the slope instability. The method is illustrated in Paranunzio et al. (2015): here we give a synthetic description of the main steps of the method, with special attention to the variations and improvements introduced in this work. Please note that, hereinafter, the term "date" is used to refer to the exact date of failure (e.g., 15 May 2004), while "day" is used for the calendar date i.e., the date without the year (e.g., 15 May).

The climate variables V to be considered for statistical analysis were selected, including the air temperature T, the variation in the air temperature ΔT (i.e., the difference in the air temperature between the day of the failure and the previous day(s)), and precipitation R. We analysed the mean air temperatures T_{mean} as in Paranunzio et al. (2015), and we also considered the minimum (T_{min}), and the maximum (T_{max}) air temperatures to obtain a more comprehensive picture of air temperature conditions before the slope failure.

- V is a time-aggregated variable, and the aggregation time must be decided. In this work, we aggregated the temperature and precipitation measurements at the daily, weekly, monthly, and quarterly scale. In other words, we calculated the average of the daily values for T_{mean}, T_{max}, T_{min}, and the cumulated values of R for 1, 7, 30, and 90 days before the date/day of failure, including the date/day of failure. With regard to ΔT, we considered time delays of 1, 3, and 6 days i.e., the difference in temperature between the date/day of the failure and the previous 1, 3 and 6 days. As an example, if the failure occurred on 15 May, ΔT_1 will be the difference in daily air temperature between 15 May and 14 May, ΔT_3 will be the difference in daily air temperature between 15 May and 12 May, ΔT_6 will be the difference in daily air temperature between 15 May and 9 May.

- The value of V for the date of the failure was then compared with a reference sample including n values, measured at the same reference meteorological station(s): we considered that a sample to be adequate for such a comparison if $n \geqslant 10$. In the ordered sample, $V_{(i)}$ is the ith value, $i=1 \ldots n$. When selecting the

Nat. Hazards Earth Syst. Sci. Discuss., doi:10.5194/nhess-2016-100, 2016
Manuscript under review for journal Nat. Hazards Earth Syst. Sci.
Published: 4 April 2016
© Author(s) 2016. CC-BY 3.0 License.

Natural Hazards and Earth System Sciences
Discussions

most suitable reference sample, we need to consider the seasonality of the climate variable. In our study area, seasonality is particularly important for the air temperature T, and we we thus compared the temperature recorded before the rockfall event with the temperature of a reference sample that included the same period. As an example, if a rockfall occurred at a given site on 15 September 2014, when we consider the average air temperature (T) in the week before the failure (i.e., the average value of T from 9 to 15 September 2014), the reference sample will include all temperature data aggregated at the weekly scale for the same period of the year i.e., the average value of T in the period from 9 to 15 September for each year in the available historical record for the same reference meteorological station. For precipitation (R) and the variation in the daily air temperature (ΔT), the reference sample is extended to include data registered in the 90-day period centred on the day of the failure (e.g., if the failure occurred on 22 November, we consider data in the previous and following 45 days, this means from 8 October to 6 January). This procedure allows obtaining a larger reference sample, and thus increases the robustness of the obtained results. This is particularly important for R, since precipitation is an intermittent process and not all years in the record necessarily have an R value recorded for the period of interest. For our analysis, we used the climate data recorded at the reference stations, and we did not transpose (extrapolate) the temperature or precipitation measurements from the meteorological station to the location (geographical position and elevation) of the detachment zone of the rockfall. In fact, the application of a constant lapse rate would merely entail a translation of all values, without affecting the estimate of the probability associated with V.

- Finally, the non-exceedance probability $P(V)$ for the climate variable V is calculated, where $P(V)=i/(n+1)$, if $V>V_{(i)}$. We hypothesize that variables with an associated $P(V)\leqslant\alpha/2$ (negative anomaly) or $P(V)\geqslant 1-\alpha/2$ (positive anomaly) can be considered relevant factors for the preparation/initiation of rockfalls (in this work, the significance level α is 0.2).

In addition to these analyses, for this work we performed a bivariate analysis to take into account additional factors that, in combination with climate anomalies, can help understanding the processes leading to slope failure. Here we give a synthetic description of the main steps of the procedure.

To describe the spatial and temporal distribution of the rockfalls listed in the inventory, we considered the following factors: (i) season of occurrence, (ii) mean elevation of the detachment zone, (iii) probability of permafrost occurrence, and (iv) magnitude of the event.

- The temporal distribution of the events was analyzed considering the season of occurrence. Rockfall events were divided in four seasonal classes i.e., Spring, Summer, Autumn, Winter. In relation to the elevation of the detachment zones, the events were divided into three classes i.e., 1500-2400 m a.s.l., 2400-3300 m a.s.l., and 3300-4200 m a.s.l. Rockfall volumes were ranked in two classes: rockfalls in the range 10^2-10^4 m^3 were classified as small events, and rockfalls in the range 10^4-10^6 m^3 were considered large events. The probability of permafrost occurrence in the detachment zone was derived from the Alpine Permafrost Index Map-APIM (Boeckli et al., 2012). APIM is defined as “a first resource to estimate permafrost conditions at any given location in the European Alps”, and it

Nat. Hazards Earth Syst. Sci. Discuss., doi:10.5194/nhess-2016-100, 2016
Manuscript under review for journal Nat. Hazards Earth Syst. Sci.
Published: 4 April 2016
© Author(s) 2016. CC-BY 3.0 License.

Natural Hazards and Earth System Sciences
Discussions

represents a static snapshot of potential permafrost distribution, as the model on which the map is based does not take into account the recent global warming. In rock, the maximal uncertainty in the elevation of the lower permafrost limit is estimated to be ±360 m. In this map, the likelihood of permafrost occurrence is classified in three classes, (i) permafrost "in nearly all conditions", (ii) "mostly in cold conditions", and (iii) "only in very favourable conditions", corresponding to a decreasing probability of permafrost occurrence. We have added the class "no permafrost" and we divided into four classes rockfall events with regard to the probability of permafrost occurrence in the detachment zone.

- Climate anomalies were grouped into five classes: (i) short-term temperature anomaly (ST) i.e., positive and negative temperature anomaly at the daily and/or weekly scale; (ii) long-term temperature anomaly (LT) i.e., positive and negative temperature anomaly at the monthly and/or quarterly scale; (iii) widespread temperature anomaly (WT) i.e, temperature anomaly distributed from the daily to the quarterly temporal range; (iv) precipitation anomaly (RT) i.e., precipitation anomaly from the weekly to the quarterly scale and (v) no climate anomaly detected (NO).

- A joint assessment of frequency distribution of climate anomalies in relation to spatio-temporal characteristics of rockfall events was performed.

5 Results

5.1 Statistical analysis of climate variables

Results of the analysis of the climate variables considered for this work are listed in Table 3. From this table, one can see that 34 (83 %) of 41 rockfalls considered in this work were associated to air temperature anomalies. For six rockfalls, a precipitation anomaly was detected, usually in combination with a temperature anomaly. The Brenva rockfall of 18 January 1997 is the only event in our catalogue that was associated solely to a precipitation anomaly. In six cases, the climate variables revealed no anomaly.

Temperature anomalies associated to rockfall occurrence were more frequently hot (53 %) than cold (35 %). In a few cases, both warm and cold temperature anomalies, at different temporal scales, were detected. Short-term temperature anomalies (ST) predominate (50 % of case studies) over long-term (LT) anomalies (15 %), but in many cases widespread temperature anomalies (WT) were detected (35 %).

Of the six rockfall events associated to a precipitation anomaly, three events were associated only to a long-term precipitation anomaly, and three events were associated to precipitation anomalies both at the weekly and at the monthly/quarterly scale.

Regarding the regional distribution of our case studies, we notice that four of the six events with no detected anomaly occurred in the Eastern Italian Alps. In the Western Italian Alps, 11 out of 19 rockfall events (58 %) were associated to warm temperature anomalies (in the short-term and/or long-term range), whereas in the Eastern Italian Alps only nine out of 21 events (43 %) were associated to warm temperature anomalies. Conversely, only five rockfalls were associated to cold temperature anomalies in

Nat. Hazards Earth Syst. Sci. Discuss., doi:10.5194/nhess-2016-100, 2016
Manuscript under review for journal Nat. Hazards Earth Syst. Sci.
Published: 4 April 2016
© Author(s) 2016. CC-BY 3.0 License.

the Western Italian Alps, and eleven in the Eastern Italian Alps. Finally, four of the six rockfall events associated with a precipitation anomaly were located in the Western Italian Alps.

5.2 Spatial and temporal distribution of rockfalls

The main characteristics of the spatial and temporal distributions of the considered events are listed in Table A1. Looking at the elevation of the detachment areas, we note that the events are evenly distributed among all elevation classes. As regards the season of occurrence, the summer events predominate and occurred mostly at elevation higher than 2400 m. All the spring events occurred at lower elevations, with the only exception of the Belvedere rockfall in April 2007. Both spring and summer events are equally distributed in the Western and Eastern sectors. Autumn events occurred mainly in the elevation range 2400-3300 m, and all have occurred in the Eastern Alps, except for the Punta Tre Amici rockfall on September 2010. Winter rockfalls are the less numerous group, they occurred all between mid-December and mid-January, and most of them are located in the Western sector of the study area.

While analysing the seasonal distribution of the events according to their volume, consider that information on the detached volume was available only for 26 rockfalls out of 41 (63 %). This is because the selected events often occurred in remote areas and caused no damage. It is likely that most of the processes for which we do not have this type of information are small-volume events ($<10^4$ m^3). Therefore, the number of small events is probably underestimated. Most of the small-volume events occurred during the summer, and none in the winter. Conversely, the large magnitude events show a quite homogeneous seasonal distribution. It is likely that the seasonal distribution of small events is influenced by the wider frequentation of mountain areas during the summer, which causes a higher probability of events and/or reporting. Finally, if we consider rockfall volumes versus elevation, we notice that small-volume events concentrate in the lower and intermediate elevation classes, while large rockfalls occurred mainly above 2400 m. The Val Formazza event of April 2009 is the only large event documented in the lower elevation class. If we analyse the case studies according to the probability of permafrost occurrence in the detachment zone, we get an information similar to that provided by the terrain elevation.

5.3 Climate anomalies and spatio-temporal distribution of rockfalls

Results of the bivariate statistical analysis are shown in Fig. 3. The climate anomalies are grouped in the five types described in Sect. 4. Note that case studies showing both *R* and *T* anomalies were counted only once, in the RT group.

Results shown in Fig. 3a highlight that half of the spring and autumn events are associated to a ST anomaly. Summer events occurred mainly in the presence of ST or WT anomalies. ST anomalies are both warm and cold, while WT anomalies are always warm. Conversely, LT anomalies, which were found only on occasion of summer events, are cold and are at the quarterly range. Winter events are associated to ST (Sass Maor, December 2011) or WT (Rocciamelone II, December 2006) anomalies, and/or to long-term *R* anomalies (Brenva, January 1997, Crammont, December 2008).

Considering to the elevation of the rockfall detachment zone (Fig. 3b), low elevation failures occurred mainly in combination with ST anomalies. Events occurred in the mid-range class (2400-3300 m a.s.l.)

Nat. Hazards Earth Syst. Sci. Discuss., doi:10.5194/nhess-2016-100, 2016
Manuscript under review for journal Nat. Hazards Earth Syst. Sci.
Published: 4 April 2016
© Author(s) 2016. CC-BY 3.0 License.

Natural Hazards and Earth System Sciences
Discussions

are homogeneously distributed among all types of anomaly. However, they are also the most numerous group of events for which no anomaly was detected. Most of the events that occurred at the highest elevations are associated to ST or WT anomalies, with warm anomalies that significantly outweigh cold ones. Interestingly, none of the failures that occurred in the highest range of elevation is exclusively associated to long-term T anomalies, or no anomaly.

With regard to the magnitude of the events (Fig. 3c**)**, there is no strong indication of a preferential distribution of small and large events among the different climate anomalies, even though small events are more numerous in the ST group, while large events are quite evenly distributed among ST, WT, and RT groups.

As for the probability of occurrence of permafrost conditions in the detachment zone, Fig. 3d shows that eight events associated to WT anomalies occurred in areas where permafrost occurrence is likely. Conversely, in non-permafrost areas events mainly concentrate across ST anomalies.

Focusing on the type of climate anomaly, we can summarize the results illustrated in Fig. 3 as follows. ST anomalies (both warm and cold) are preferentially associated to small-volume failures, occurring in any season at lower elevations (where no permafrost is expected). Only few events are associated uniquely to LT anomalies, which resulted to be always cold and at the quarterly range, and occurred during the summer. These events are located in the lower or medium range of elevation, where permafrost is absent or present only in cold conditions. WT anomalies (mainly of the warm type) are associated in particular to summer events, occurring at high elevation (in particular in the highest altitudes, where permafrost is present in all conditions) and that involve large volumes of rock. RT anomalies are associated to failures occurring in almost any season, of both small and large magnitude, mainly in the medium range of elevation, in variable permafrost conditions. Case studies associated to NO anomaly are mainly reported during the summer, at low or medium elevations.

6 Discussion

In this work, we used a modified version of the statistical method proposed by Paranunzio et al. (2015), which can be easily applied to diverse climate and geographical settings, and to any type of natural instability. This method provides a first screening of the climate parameters that might have contributed to slope failure occurrence. In this light, the most relevant outcomes of our analyses on a sample of 41 recent rockfalls in the Italian Alps can be synthetized as follows:

(i) In 85 % of our case studies, one (or more) climate anomaly was identified in association with rockfall occurrence;

(ii) Most of the rockfall events were associated with a temperature anomaly (34 cases out of 41). In most cases (30 out of 34) it was a short-term temperature anomaly, occasionally (12 cases) combined with a long-term temperature anomaly;

(iii) Surprisingly, temperature anomalies associated with rockfall occurrence were positive and/or negative, with only a slight prevalence of the positive anomalies;

Nat. Hazards Earth Syst. Sci. Discuss., doi:10.5194/nhess-2016-100, 2016
Manuscript under review for journal Nat. Hazards Earth Syst. Sci.
Published: 4 April 2016
© Author(s) 2016. CC-BY 3.0 License.

(iv) Only six rockfalls (15 %) were associated to exceptional precipitations in the medium/long term (i.e., 7-90 days before the failure);

(v) Timing and conditions of rockfall initiation differ in relation to the elevation altitude. At lower elevation (1500-2400 m), rockfalls occurred mainly in spring, and were mostly associated to negative temperature anomalies. At medium elevation (2400-3300 m), rockfall events concentrated in summer and positive temperature anomalies prevail on the negative anomalies. In this altitudinal range, we find the largest number of events not associated to climate anomaly. Summer events prevail also at the highest elevations (>3300 m), mostly in association with positive temperature anomalies;

(vi) In the Western Alps, rockfalls associated with warm air temperatures predominate, whereas in the Eastern Alps rockfalls are often associated to very cold conditions.

At higher altitude (above 3300 m) rockfalls documented since 2003 were mainly associated to positive temperature anomalies. At lower altitudes, the impact of climate change on slope stability, if it exists, must be sought in more complex processes (e.g., change of the snow/rain ratio, increased temperature variability with more frequent cycles of snowfall/snowmelt and of freeze/thaw in the rock slopes).

Looking to regional differences, rockfall occurrence in the Western Alps can be attributed to the build-up of water pressure in the rock masses due to accelerated snowmelt and/or permafrost thaw. In the Eastern Alps, instead, water pressure increase inside the slopes may be related to freezing of water springs along the slopes, and/or by repeated cycles of snowfall/snowmelt, especially in autumn. The differences can be ascribed to the typical topographic settings of the two sectors. In particular, the Western Italian Alps host the highest peaks in the study area (e.g., Mont Blanc, 4810 m, Monte Rosa, 4637 m, Matterhorn 4478 m), where we expect permafrost in all conditions. Peak elevation in the Eastern Alps is much lower (Tofana di Mezzo, 3245 m, Sorapiss, 3205 m, Cima Undici, 3092 m) and permafrost is expected only in cold or favourable conditions.

By analysing the type of the detected climate anomaly(ies) in combination with spatio-temporal characteristics of the individual rockfalls, we attempted to provide some possible explanation on the temperature-related processes that may have caused the slope failures. Details on this case-by-case analysis are listed in Table A1, below we give general comments:

(i) Permafrost thawing, necessarily related to a long-term positive temperature anomaly, seems to contribute to slope failure only at the highest elevations (>3300 m), and only as a predisposing factor. No event in our catalogue occurred in association solely with a long-term, positive thermal anomaly.

(ii) Positive ST anomalies may have contributed to rockfall triggering in multiple ways. In spring and early summer, they may have caused accelerated snowmelt (Cardinali et al., 2000). In summer, they may have accelerated the ongoing process of permafrost thaw. In autumn, warm temperatures may have caused melting of an early snowfall, or precipitation to fall as rain rather than as snow. More complex is the interpretation of the role of the positive ST anomalies that are

Nat. Hazards Earth Syst. Sci. Discuss., doi:10.5194/nhess-2016-100, 2016
Manuscript under review for journal Nat. Hazards Earth Syst. Sci.
Published: 4 April 2016
© Author(s) 2016. CC-BY 3.0 License.

usually associated to winter events. In these cases, it is likely that temperature, though higher than the average, was well below 0 °C at the time of failure;

(iii) Negative ST anomalies may have been responsible for rockfall triggering by freezing the water springs along the slope, thus causing the blockage of ground water flow and the build-up of water pressure in the rock masses leading to slope failure (MacSaveney and Massey, 2013).

In order to properly consider the outcomes of this study, some important constraints of our work have to be kept in mind. Our method may not have detected all possible climate anomalies associated with the onset of the slope failures. To refine the results, or to use the method for different purposes or in different geographic settings, the method can be composed and/or integrated with further variables and analysis, e.g. considering different temporal aggregations scales.

Our method is not an operational tool for landslide (rockfall) forecasting i.e., it does not provide thresholds for rockfall initiation. In order to do so, it would need to be further validated on a larger dataset, and with a false positive analysis, i.e. the analysis of the number of times that a climate anomaly was detected and no slope instability occurred. However, this validation could prove difficult for high elevation areas, where slope failures are only seldom reported. Our method is instead intended as a tool for assessing the possible role of climate parameters in slope failure occurrence.

The sample size that we used for this work is limited from a statistical point of view. This is due in part to the fact that the landslides that we are looking at i.e., rockfalls occurring at high elevation and not triggered by rainfall, earthquakes or human activities, are only a small subset of all landslides occurring in the Italian Alps (see e.g., Stoffel et al., 2014, Brunetti et al., 2015). In addition, the acquisition of information about slope failures in remote areas such as high mountains is often difficult. Since our main requirements while collecting data for our study were the knowledge of the failure date and of the (at least indicative) location of the detachment zone, together with the availability of climate records covering the failure date, only part of the rockfall events that we collected could be used for this work.

Moreover, we know that our dataset includes inhomogeneities. Small-volume events are usually reported only if they caused some relevant damage and, for this reason, they are probably underrepresented in the dataset. Summer events are documented more easily than those occurring in the other seasons. Many of the documented rockfalls occurred in the most famous mountain ranges (Mont-Blanc, Monte Rosa, Dolomites), and this is due in part to the high frequentation and to increased media attention in these mountains. Finally, many news come from newspapers and may contain inaccuracies, which are not always simple to identify and connect.

However, we point out that only a few inventories of this type are available in the literature, and their size is comparable to our dataset (Noetzli et al., 2003; Ravanel et al., 2010; Allen et al., 2011; Fischer et al., 2012; Allen and Huggel, 2013). Data collected in the inventories are the result of years of documentation, field surveys and remote sensing. It is unlikely that the number of events listed in the catalogue will increase substantially in the next few years, considered the remoteness and the low frequentation of high mountains, unless new techniques will become available to support this type of studies (e.g., Manconi et al., 2015). The straightest way to overcome these difficulties would be the combination of datasets from

Nat. Hazards Earth Syst. Sci. Discuss., doi:10.5194/nhess-2016-100, 2016
Manuscript under review for journal Nat. Hazards Earth Syst. Sci.
Published: 4 April 2016
© Author(s) 2016. CC-BY 3.0 License.

different mountain areas of the world. This approach would give more strength and robustness to the statistical analysis, even if one will always inevitably cope with small numbers of case studies, compared to other types of processes, or other geographic settings. Moreover, merging catalogues from different sources would require that the collection of geologic and climate data is done according to common standards. This is not the case at the moment, despite a few attempts in this direction conducted in the framework of international projects (e.g., Deline et al., 2007).

7 Conclusions

The statistical method used in this work proved to be a valuable tool to discriminate whether, and which climate variables may have contributed to rockfall triggering at high elevation in recent years. The schematic nature and the simplicity of the method are, in our view, also its main strength, as the method can be applied to a wide range of climate parameters, to any process of instability, and in any geographical context.

Our results show that, in absence of a clear rainfall trigger, temperature is a key factor controlling rockfall occurrence in the Italian Alps. Temperature control is more evident in the short term and at higher elevation, where the prevalence of warm temperature anomalies in association to slope failures supports the hypothesis of an impact of global warming on slope stability, as a consequence of cryosphere degradation. Our study also demonstrates that the type of temperature anomaly, and thus how temperature controlled rockfall occurrence, was very different from case to case. Warm temperatures could enhance permafrost thaw and snowmelt at higher altitudes or cause melting of early snowfall at lower elevation. Cold temperature anomalies may cause the blockage of groundwater flow and the build-up of high water pressures inside the rock mass. Some interesting insights could be made on the spatial distribution of the anomalies: rockfalls in the Eastern Alps are mainly related to cold temperature anomalies, while in the Western Alps slope failures are mainly associated with warm temperature anomalies.

In conclusion, the approach used in this study allowed to define the climate signature of the considered slope failures. A bottom-up assessment of the role of climate variables in the development of a set of slope failure events, as we did in this work, is an essential step towards a characterization and a quantification of the impacts of climate change on slope instability in mountain areas, and for the definition of hazard scenarios under the present climate trend.

Acknowledgments

This research was conducted with funding provided by the Italian National Department for Civil Protection (DPC) in the framework of a CNR IRPI project. FL and RP acknowledge support from the ERC project CoG 647473. We thank ARPA Piemonte, ARPA Lombardia, ARPA Veneto, Centro Funzionale - Regione Autonoma Valle d'Aosta, Ufficio Idrografico - Provincia Autonoma di Bolzano and Meteotrentino for providing access to their climate databases.

Nat. Hazards Earth Syst. Sci. Discuss., doi:10.5194/nhess-2016-100, 2016
Manuscript under review for journal Nat. Hazards Earth Syst. Sci.
Published: 4 April 2016
© Author(s) 2016. CC-BY 3.0 License.

Natural Hazards and Earth System Sciences
Discussions

References

Allen, S. K., Cox, S. C., and Owens, I. F.: Rock avalanches and other landslides in the central Southern Alps of New Zealand: a regional study considering possible climate change impacts, Landslides, 8, 33–48, 2011.

Allen, S. and Huggel, C.: Extremely warm temperatures as a potential cause of recent high mountain rockfall, Glob. Planet. Change, 107, 59–69, 2013.

ARPA Piemonte: Evento meteopluviometrico del 26-28 aprile 2009, 2009.

Auer, I., Bohm, R., Jurkovic, A., Lipa, W., Orlik, A., Potzmann, R., Schoner, W., Ungersbock, M., Matulla, C., Briffa, K., Jones, P., Efthymiadis, D., Brunetti, M., Nanni, T., Maugeri, M., Mercalli, L., Mestre, O., Moisselin, J. M., Begert, M., Muller-Westermeier, G., Kveton, V., Bochnicek, O., Stastny, P., Lapin, M., Szalai, S., Szentimrey, T., Cegnar, T., Dolinar, M., Gajic-Capka, M., Zaninovic, K., Majstorovic, Z., and Nieplova, E.: HISTALP - historical instrumental climatological surface time series of the Greater Alpine Region, Int. J. Climatol., 27, 17–46, 2007.

Barla, G., Dutto, F., and Mortara, G.: Brenva glacier rock avalanche of 18 January 1997 on the Mount Blanc range, northwest Italy, Landslide News, 13, 2-5, 2000.

Barry, R. G.: Mountain Weather and Climate, 3rd edn, Cambridge University Press, New York, 2008.

Boeckli, L., Brenning, A., Gruber, S., and Noetzli, J.: Permafrost distribution in the European Alps: Calculation and evaluation of an index map and summary statistics, Cryosphere, 6(c), 807–820, 2012.

Beniston, M.: Mountain weather and climate: A general overview and a focus on climatic change in the Alps, Hydrobiologia, 562, 3–16, 2006.

Brunetti, M., Lentini, G., Maugeri, M., Nanni, T., Auer, I., Bohm, R., and Schoner, W.: Climate variability and change in the Greater Alpine Region over the last two centuries based on multi-variable analysis, Int. J. Climatol., 29, 2197–2225, 2009.

Brunetti, M. T., Peruccacci, S., Rossi, M., Luciani, S., Valigi, D., and Guzzetti, F.: Rainfall thresholds for the possible occurrence of landslides in Italy, Nat. Hazards Earth Syst. Sci., 10, 447–458, 2010.

Cardinali, M., Ardizzone, F., Galli, M., Guzzetti, F., and Reichenbach, P.: Landslides triggered by rapid snow melting: the December 1996–January 1997 event in Central Italy, in: Proceedings 1st Plinius Conference on Mediterranean Storms, Maratea, Italy, 14-16 October 1999, 439–448, 2000.

Chiarle, M. and Mortara, G.: Geomorphological impact of climate change on alpine glacial and periglacialareas. Examples of processes and description of research needs, in: Interpraevent 2008 conference proceedings, Dornbirn, Austria, 26-30 May 2008, vol 2, 111–122, 2008.

Chiarle, M., Paranunzio, R., Laio, F., Nigrelli, G., and Guzzetti, F.: Recent slope failures in the Dolomites (Northeastern Italian Alps) in a context of climate change, EGU General Assembly, Vienna, Austria, 27 April–2 May, EGU2014-4017, 2014

Deline, P., Kirkbride, M. P., Ravanel, L., and Ravello, M.: The Tré-la-Tête rockfall onto the Lex Blanche Glacier, Mont Blanc Massif, Italy, in September 2008, Geogr. Fis. e Din. Quat., 31(2), 251–254, 2008.

Deline, P., Chiarle, M., Curtaz, M., Kellerer-Pirklbauer, A., Lieb, G. K., Mayr, V., Mortara, G., and Ravanel L.: Chapter 3: Rockfalls, in: Hazards related to permafrost and to permafrost degradation,

© Author(s) 2016. CC-BY 3.0 License.

PermaNET project, state-of-the-art report 6.2, Schoeneich, P., Dall'Amico, M., Deline, P., and Zischg A. (Eds.), on-line publication ISBN 978-2-903095-59-8, 67-105, 2011.

Deline, P., Broccolato, M., Noetzli, J., Ravanel, L., and Tamburini, A.: The December 2008 Crammont Rock avalanche, Mont Blanc Massif Area, Italy, in Landslide Science and Practice: Global Environmental Change, vol. 4, pp. 403–408, 2013.

Esposito, S., Alilla, R., Beltrano, M. C., Dal Monte, G., Di Giuseppe, E., Iafrate, L., Libertà, A., Parisse, B., Raparelli, E., and Scaglione, M.: Atlante italiano del clima e dei cambiamenti climatici, Progetto Agroscenari, Consiglio per la Ricerca e la Sperimentazione in Agricoltura, Unità di Ricerca per la Climatologia e la Meteorologia applicate all'Agricoltura, 29-30 October 2014, Rome, Italy, 2014.

Fischer, L., Purves, R. S., Huggel, C., Noetzli, J. and Haeberli, W.: On the influence of topographic, geological and cryospheric factors on rock avalanches and rockfalls in high-mountain areas, Nat. Hazards Earth Syst. Sci., 12, 241–254, doi:10.5194/nhess-12-241-2012, 2012.

Gruber, S., Hoelzle, M., and Haeberli, W.: Permafrost thaw and destabilization of Alpine rock walls in the hot summer of 2003, Geophys. Res. Lett., 31, 4, doi:10.1029/2004gl020051, 2004.

Gruber, S. and Haeberli, W.: Permafrost in steep bedrock slopes and its temperatures-related destabilization following climate change, J. Geophys. Res. Earth Surf., 112, doi:10.1029/2006JF000547, 2007.

Guzzetti, F., Peruccacci, S., Rossi, M., and Stark, C. P.: The rainfall intensity-duration control of shallow landslides and debris flows: An update, Landslides, 5, 3–17, doi:10.1007/s10346-007-0112-1, 2008.

Harris, C., Arenson, L. U., Christiansen, H. H., Etzemuller, B., Frauenfelder, R., Gruber, S., Haeberli, W., Hauck, C., Holzle, M., Humlum, O., Isaksen, K., Kaab, A., Kern-Lutschg, M. A., Lehning, M., Matsuoka, N., Murton, J. B., Nozli, J., Phillips, M., Ross, N., Seppala, M., Springman, S. M., and Muhll, D. V: Permafrost and climate in Europe: Monitoring and modelling thermal, geomorphological and geotechnical responses, Earth-Science Rev., 92, 117–171, , doi:10.1016/j.earscirev.2008.12.002, 2009.

Huggel, C., Salzmann, N., Allen, S., Caplan-Auerbach, J., Fischer, L., Haeberli, W., Larsen, C., Schneider, D., and Wessels, R.: Recent and future warm extreme events and high-mountain slope stability, Philos. Trans. R. Soc. a-Mathematical Phys. Eng. Sci., 368, 2435–2459, doi:10.1098/rsta.2010.0078, 2010.

Huggel, C., Carey, M., Clague, J. J., and Kääb, A. (Eds.): The High-Mountain Cryosphere, Cambridge University Press, 376 pp, 2015.

Manconi, A., Coviello, V., De Santis, F., and Picozzi, M.: Near real-time detection and characterization of landslides using broadband seismic networks, EGU General Assembly, Vienna, Austria, 12–17 April 2015, EGU2015-11288, 2015.

McSaveney, M. and Massey, C.: Did radiative cooling trigger New Zealand's 2007 Young River landslide?, in: Margottini, C., et al. (Eds.), Landslide Science and Practice, Springer Berlin Heidelberg, G347-353, 2013.

Mortara, G. and Tamburini, A. (Eds.): Il ghiacciaio del Belvedere e l'emergenza del lago Effimero, Edizioni Società Meteorologica Subalpina, Castello Borello, Bussoleno, 192 pp, 2009.

Nat. Hazards Earth Syst. Sci. Discuss., doi:10.5194/nhess-2016-100, 2016
Manuscript under review for journal Nat. Hazards Earth Syst. Sci.
Published: 4 April 2016
© Author(s) 2016. CC-BY 3.0 License.

Natural Hazards and Earth System Sciences
Discussions

Nigrelli, G., Lucchesi, S., Bertotto, S., Fioraso, G., and Chiarle, M.:Climate variability and Alpine glaciers evolution in Northwestern Italy from the Little Ice Age to the 2010s, Theoretical and Applied Climatology, 122(3-4), 595-608, 2015.

Noetzli, J., Hoelzle, M., and Haeberli, W.: Mountain permafrost and recent Alpine rock-fall events: a GIS-based approach to determine critical factors, Permafrost, 2, 827–832, 2003.

Paranunzio, R., Laio, F., Nigrelli, G., and Chiarle, M.: A method to reveal climatic variables triggering slope failures at high elevation, Nat. Hazards, 2014.

Ravanel, L., Allignol, F., Deline, P., Gruber, S., and Ravello, M.: Rock falls in the Mont Blanc Massif in 2007 and 2008, Landslides, 7(4), 493–501, 2010.

Schar, C., Vidale, P. L., Luthi, D., Frei, C., Haberli, C., Liniger, M. A., and Appenzeller, C.: The role of increasing temperature variability in European summer heatwaves, Nature, 427(6972), 2004.

Sosio, R., Crosta, G. B., and Hungr, O.: Complete dynamic modeling calibration for the Thurwieser rock avalanche (Italian Central Alps), Eng. Geol., 100(1-2), 11–26, 2008.

Stocker, T. F., Qin, D., Plattner, G.-K., Tignor, M., Allen, S. K., Boschung, J., Nauels, A., Xia, Y., Bex, V., and Midgley, P. M.: IPCC, 2013: Climate Change 2013: The Physical Science Basis. Contribution of Working Group I to the Fifth Assessment Report of the Intergovernmental Panel on Climate Change, IPCC, AR5, 1535, 2013.

Stoffel, M., Tiranti, D., and Huggel, C.: Climate change impacts on mass movements--case studies from the European Alps., Sci. Total Environ., 493, 1255–66, 2014.

Tamburini, A., Villa, F., Fischer, L., Hungr, O., Chiarle, M., and Mortara, G.: Slope instabilities in high-mountain rock walls. Recent events on the Monte Rosa east face (Macugnaga, NW Italy), in Landslide Science and Practice: Spatial Analysis and Modelling, vol. 3, pp. 327–332, 2013.

Turconi, L., Kumar De, S., Tropeano, D., and Savio, G.: Slope failure and related processes in the Mt. Rocciamelone area (Cenischia Valley, Western Italian Alps), Geomorphology, 114, 115–128, 2010.

WMO (World Meterological Organization): Guide to climatological practices (WMO-No. 100), 3rd edn., Geneva, 180 pp., 2011.

Zemp, M., Haeberli, W., Hoelzle, M., and Paul, F.: Alpine glaciers to disappear within decades?, Geophys. Res. Lett., 33, 2006.

Nat. Hazards Earth Syst. Sci. Discuss., doi:10.5194/nhess-2016-100, 2016
Manuscript under review for journal Nat. Hazards Earth Syst. Sci.
Published: 4 April 2016
© Author(s) 2016. CC-BY 3.0 License.

Natural Hazards and Earth System Sciences
Discussions

1 **Tables**

2 Table 1. Main characteristics of the rockfalls and rock-avalanches considered in this inventory. Events are listed
3 in chronological order. Wherever available, references have been reported. Cited references are: Barla et al.,
4 2000 [a], Deline et al., 2008 [b], Turconi et al., 2010 [c], Fischer et al., 2011 [d], Tamburini et al., 2013 [e],
5 Fischer et al., 2013 [f], Sosio et al., 2008 [g], Chiarle et al., 2014 [h], ARPA, 2009 [i].
6

No.	Location	Date and time of occurrence		Location				Volume	Reference
				Elevation	Latitude	Longitude	Aspect		
		(dd month yyyy)	(UTC)	(m a.s.l.)	N	E		(m^3)	
	Western Italian Alps								
1	Brenva	18 January 1997	-	3725	45°50'10"	6°53'0.76"	SE	$2x10^6$	[a]
2	Matterhorn I	4 August 2003	night	3880	45°58'24.9"	7°38'54.67"	SW	10^2x10^3	[b]
3	Matterhorn II	18 August 2003	16:00	3770	45°58'22.28"	7°38'48.96"	SW	$2x10^3$	[b]
4	Mont Pelà	19 July 2004	-	2340	45°36'12.61"	7° 2'12.91"	E	$3x10^2$	-
5	Matterhorn III	18 July 2005	15:30	3715	5°58'16.17"	7°38'36.21"	NW	-	[b]
6	Rocciamelone I	29 July 2005	-	3100-3250	45°11'51"	7°04'30"	W	-	[c]
7	Matterhorn IV	25 July 2006	16:00	3750	45°58'22.57"	7°38'49.02"	SW	-	[b]
8	Rocciamelone II	26 December 2006	-	3100-3250	45°11'51"	7°04'30"	W	$>10^4$	[c]
9	Belvedere	21 April 2007	10:00	4200	45°56'3.05"	7°52'36.96"	E	$1.5x10^5$	[d] [e]
10	Tré-la-Tête	11 September 2008	7:00	3470	5°47'27.35"	6°49'29.52"	E	10^4x10^5	[b]
11	Punta Patri Nord	18 September 2008	7:45	3200-3400	45°32'31.72"	7°21'40.22"	E	$1x10^5$	[b]
12	Crammont	24 December 2008	16:21	2400-2450	45°46'6.53"	6°56'16.24"	N	$5x10^5$	[b]
13	Val Formazza	19 April 2009	9:00	1950	46°23'31.10"	8°27'16.58"	NW	10^5-10^6	[i]
14	Monviso	26 July 2009	12:00	3133	44°39'24.21"	7° 6'2.29"	E	$2x10^3$	-
15	Mont Rouge Peuterey	13 August 2009	13:00	2941	45°48'14.67"	6°53'52.45"	SE	-	-
16	Matterhorn V	28 August 2009	during the day	3880	45°58'24.49"	7°38'54.67"	SW	-	-
17	Melezet	21 May 2010	18:40	1500	45°3'29.83"	6°40'37.18"	E	$2x10^3$	-
18	Punta Tre Amici	26 September 2010	late morning	3425	45°55'31.88"	7°54'27.50"	NE	$1x10^5$	[f]
19	Gressoney-Saint-Jean	2 May 2013	late afternoon	2000	45°47'25.44"	7°48'40.37"	E	10^2-10^3	-
	Central and Eastern Italian Alps								
20	Latemar	15 August 2000	17:20	2799	46°34'38.22"	11°50'18.6"	-	-	-
21	San Vito di Cadore	30 October 2003	15:00	2460	46°29'24.06"	12°13'13.2"	W	$5x10^3$	-
22	Colcuc	2 April 2004	1:30	1700-1800	46°27'18.15"	12°0'9.46"	W	10^3-10^4	-
23	Ivigna	24 May 2004	afternoon	2050	46°41'33.17"	11°15'24.58"	-	-	-
24	Torre Trephor	13 June 2004	-	>2000	46°30'37.81"	12°3'8.83"	NE	-	-
25	Cima Dodici I	1 July 2004	night	3094	46°37'6"	12°21'36.96	W	-	-
26	Forcella dei Ciampei	1 July 2004	night	2366	46°34'38.22"	11°50'18.64"	N	10^2	-
27	Monte Pelmo	19 August 2004	16:00	2900	46°25'6.75"	12°7'54.95"	-	-	-
28	Thurwieser	18 September 2004	13:41	3658	46°29'42.81"	10°31'32.23"	S	$2\text{-}2.5x10^6$	[g]
29	Monte Castelin	21 September 2004	7:00	1580	46°20'56.00"	12°15'12.00"	W	-	-
30	Tofana di Rozes	17 August 2005	13:00	2656	46°32'3.56"	12° 2'32.33"	SE	-	-
31	Monte Pelf	23 April 2006	8:00	1400-1500	46°24'56.00"	12°8'9.00"	N	-	-
32	Cima Dodici II	20 July 2006	10:00	3094	46°37'6"	12°21'36.96	W	$1x10^5$	-
33	Cima Una	12 October 2007	8:39	2598	46°38'23.63"	12°20'57.70"	N	$6x10^4$	-
34	Cima Canali	19 August 2008	11:45	2850	46°14'38.22"	11°51'49.31"	S	$3x10^3$	-
35	Cima Undici	31 August 2008	afternoon	3092	46°38'8.09"	12°22'46.30"	-	$3x10^2$	-
36	Plattkofel	19 August 2010	15:00	2650	45°32'31.72"	7°21'40.22"	NE	$7x10^2$	[b]
37	Euringer	11 August 2011	6:30	2394	46°31'28.01"	11°34'19.56"	NE	$2x10^3$	-
38	Sass Maor	21 December 2011	6:23	2200	46°14'5.64"	11°51'4.05"	E	-	-
39	Sorapiss	30 September 2013	21:00	3150	46°31'50.90"	12°13'1.14"	N	$4.7x10^3$	[h]
40	Monte Civetta	16 November2013	14:20	2600	46°22'41.18"	12°2'20.26"	NW	$5x10^4$	[h]
41	Antelao	22 November 2013	-	2050-2250	46°27'0.13"	12°14'30.52"	SW	-	[h]

Nat. Hazards Earth Syst. Sci. Discuss., doi:10.5194/nhess-2016-100, 2016
Manuscript under review for journal Nat. Hazards Earth Syst. Sci.
Published: 4 April 2016
© Author(s) 2016. CC-BY 3.0 License.

Natural Hazards and Earth System Sciences
Discussions

Table 2. Main characteristics of the meteorological stations considered in this study. Only meteorological stations representing the best compromise between the requirements mentioned in Sect. 3.2 (i.e., covering the failure date, long-term dataset, low distance from the failure area) are displayed. No.: failure point numbers (from Table 1) associated to the meteorological stations; variables recorded at the stations: *T* (temperature), *ΔT* (temperature variation between the day of the failure and the days before) and *R* (precipitation). Data source: ARPA Piemonte, 2014 (PIE); ARPA Veneto, 2014 (VEN); Centro Funzionale – Regione Autonoma Valle d'Aosta, 2014 (VDA); Ufficio Idrografico - Provincia Autonoma di Bolzano, 2014 (BUI); Meteotrentino, 2014 (MET).

Station name	Location			Observation period	Data source	Failure point
	Elevation (m a.s.l.)	Latitude (N)	Longitude (E)	(years)		(No.)
Western Italian Alps						
Barcenisio	1525	45°11'30.34"	6°59'6.05"	1994-2013	PIE	6-8
Formazza-Bruggi	1226	46°20'51.60"	8°25'43.67"	1999-2013	PIE	13
Gressoney-Saint-Jean-Weissmatten	2038	45°44'54.41"	7°49'30.26"	2003-2013	VDA	19
Cogne-Lillaz	1613	45°35'43.03"	7°23'29.19"	2002-2012	VDA	11
Lex Blanche	2162	45°45'58.86"	6°50'17.84"	2002-2012	VDA	15
Passo del Moro	2820	45°59'53"	7°58'39	1988-2014	PIE	9-18
Pontechianale	1575	44°36'43.02"	7°03'9.07"	1993-2013	PIE	14
Prerichard	1353	45°4'29.91"	6°42'59.17"	1990-2013	PIE	17
Pré-Saint-Didier-Plan Praz	2044	45°45'28.76"	6°57'9.71"	1993-2012	VDA	1-10-12
Valgrisenche-Menthieu	1859	45°34'0.24"	7°12'30.19"	2001-2012	VDA	4
Valtournenche-Lago Goillet	2526	45°55'53.52"	7°39'45.46"	1942-2012	VDA	2-3-5-7-16
Eastern Italian Alps						
Campo di Zoldo	884	46°20'47.68"	12°11'3.14"	1993-2013	VEN	29
Caprile	1008	46°26'25.35"	11°59'24.13"	1993-2013	VEN	22-40
Corvara in Badia	1558	46°33'1.48"	11°52'23.71"	1956-2013	BUI	26
Faloria	2240	46°31'38.53"	12°10'30.22"	1993-2013	VEN	21-39-41
Fié allo Sciliar	840	46°30'48.24"	11°30'21.60"	1980-2013	BUI	37
Passo Falzarego	2090	46°31'7.20"	12°00'24.51"	1993-2013	VEN	24-26-30
Passo Rolle	2012	46°17'52.70"	11°47'13.10"	1980-2013	MET	34-38
Passo Costalunga	1750	46°24'18.27"	11°35'9.16"	1991-2012	MET	20
Passo Monte Croce Comelico	2150	44°41'21.99"	07°07'42.93"	1993-2013	VEN	25-32-33-35
Passo Valles	2032	46°20'18.20"	11°47'59.20"	1985-2013	MET	36-37
Sarentino	966	46°38'26.16"	11°21'18.36"	1977-2013	BUI	23
Selva Gardena	1570	46°32'44.16"	11°46'6.24"	1991-2013	BUI	36
Soffranco	605	46°16'41.03"	12°14'33.74"	1993-2013	VEN	31
Solda	1907	46°30'55.03"	10°35'52.53"	1971-2013	BUI	23-28
Solda Cima Beltovo	3328	46°30'10.37"	10°37'42.91"	1998-2013	BUI	28
Villanova (Borca di Cadore)	968	46°26'35.58"	12°12'22.52"	1993-2013	VEN	27

Nat. Hazards Earth Syst. Sci. Discuss., doi:10.5194/nhess-2016-100, 2016
Manuscript under review for journal Nat. Hazards Earth Syst. Sci.
Published: 4 April 2016
© Author(s) 2016. CC-BY 3.0 License.

Natural Hazards and Earth System Sciences
Discussions

Table 3. Estimation of the non-exceedance probability P(V) associated with the variable V, where V may be temperature (T), precipitation (R) or temperature variation between the day of the failure and the days before (ΔT), and V is the correspondent value recorded when the failure occurred. The aggregation range is reported, i.e. daily range (d), weekly range (7d), monthly range (30d) and quarterly range (90d) for T and R, while ΔT refers to the previous day (-1d), three (-3d) and 6 days (-6d) before failure. Probability values related to T and ΔT are reported in each row referring to the mean, maximum and minimum temperature, in this order. The symbols ">" and "<" have been used when the values have been extrapolated. "NA" refers to an available data. The symbol "/" has been used when no precipitation have been recorded. Variables characterized by P(V)$\leqslant\alpha/2$ or P(V)$\geqslant$1-$\alpha/2$ (here α=0.2) are highlighted respectively in light blue and yellow (for R, we only report P(V)$\geqslant$1-$\alpha/2$).

No.	Location	Variables	Temporal aggregation						
			1d	7d	30d	90d	-1d	-3d	-6d
	Western Italian Alps								
1	Brenva	T	0.58 0.61 0.62	0.80 0.75 0.82	0.25 0.29 0.33	0.45 0.38 0.54			
		ΔT					0.24 0.21 0.24	0.20 0.16 0.20	0.43 0.44 0.43
		R	/	0.78	0.67	0.91			
2	Matterhorn I	T	0.94 0.94 0.96	0.72 0.74 0.62	0.93 0.93 0.86	0.95 0.89 0.94			
		ΔT					0.64 0.56 0.84	0.98 0.99 0.93	0.77 0.78 0.77
		R	/	0.22	0.02	0.17			
3	Matterhorn II	T	0.80 0.49 0.75	0.97 0.94 0.97	0.95 0.92 0.95	0.96 0.96 0.98			
		ΔT					0.33 0.27 0.64	0.24 0.35 0.20	0.20 0.23 0.24
		R	0.65	0.35	0.18	0.18			
4	Mont Pelà	T	0.26 0.17 0.55	0.27 0.29 0.27	0.12 0.13 0.12	<0.09 <0.09 <0.09			
		ΔT					0.25 0.21 0.29	0.29 0.15 0.42	0.83 0.69 0.85
		R	0.72	0.80	0.68	<0.08			
5	Matterhorn III	T	0.94 0.93 0.97	0.78 0.74 0.80	0.76 0.76 0.75	0.71 0.72 0.69			
		ΔT					0.75 0.83 0.62	0.84 0.74 0.93	0.94 0.97 0.89
		R	/	0.18	0.27	0.41			
6	Rocciamelone I	T	0.88 0.35 >0.94	0.49 0.45 0.63	0.55 0.57 0.58	0.85 0.85 0.85			
		ΔT					0.21 0.12 0.45	0.67 0.41 0.78	0.86 0.67 0.93
		R	/	0.05	0.19	0.20			
7	Matterhorn IV	T	0.98 0.94 0.96	0.93 0.94 0.90	0.93 0.91 0.91	0.81 0.78 0.76			
		ΔT					0.64 0.56 0.84	0.58 0.54 0.69	0.80 0.78 0.84
		R	0.15	0.70	0.70	0.47			
8	Rocciamelone II	T	>0.94 0.85 >0.94	0.65 0.65 0.69	>0.94 >0.94 >0.94	>0.94 >0.94 >0.94			
		ΔT					0.25 0.27 0.11	0.59 0.70 0.74	0.83 0.88 0.87
		R	/	0.40	0.63	0.36			
9	Belvedere	T	>0.96 >0.96 >0.96	>0.93 >0.93 >0.93	0.89 0.90 0.90	0.81 0.82 0.81			
		ΔT					0.63 0.71 0.79	0.72 0.80 0.62	0.43 0.47 0.56
		R	/	/	0.54	0.40			
10	Tré-la-Tête	T	0.88 0.61 >0.95	0.70 0.59 0.70	0.48 0.57 0.48	0.66 0.63 0.67			
		ΔT					0.13 0.21 0.17	0.79 0.55 0.93	0.75 0.67 0.87
		R	0.46	0.63	0.79	0.95			
11	Punta Patri Nord	T	0.21 NA NA	<0.09 NA NA	0.31 NA NA	0.36 NA NA			
		ΔT					0.81 NA NA	0.79 NA NA	0.07 NA NA
		R	0.37	0.73	0.61	0.55			
12	Crammont	T	0.92 >0.95 0.93	>0.95 >0.95 >0.95	0.30 0.31 0.37	0.66 0.63 0.67			
		ΔT					0.22 0.13 0.22	0.59 0.67 0.59	0.94 0.94 0.94
		R	/	0.87	0.51	0.91			
13	Val Formazza	T	0.28 0.32 0.74	0.60 0.68 0.38	0.50 0.67 0.56	0.38 0.35 0.33			
		ΔT					0.23 0.05 0.89	0.67 0.59 0.65	0.18 0.14 0.42
		R	0.31	0.21	0.58	0.46			
14	Monviso	T	0.25 0.31 0.15	0.57 0.32 0.55	0.46 0.43 0.43	0.85 0.86 0.56			
		ΔT					0.15 0.29 0.24	0.36 0.69 0.11	0.57 0.53 0.69
		R	/	/	0.19	0.50			
15	Mont Rouge Peuterey	T	0.83 0.77 0.84	0.77 0.75 0.82	0.67 0.80 0.69	0.83 0.83 0.83			
		ΔT					0.59 0.34 0.31	0.84 0.76 0.63	0.46 0.58 0.66
		R	/	0.64	0.38	0.36			
16	Matterhorn V	T	0.84 0.80 0.88	0.83 0.80 0.91	0.93 0.93 0.93	0.88 0.87 0.88			
		ΔT					0.83 0.91 0.64	0.35 0.45 0.30	0.34 0.39 0.34
		R	/	0.71	0.62	0.34			
17	Melezet	T	0.67 0.75 0.34	0.18 0.22 0.20	0.27 0.30 0.28	0.14 0.13 0.18			
		ΔT					0.72 0.74 0.86	0.72 0.90 0.31	0.90 0.95 0.72
		R	/	0.12	0.62	0.29			
18	Punta Tre Amici	T	<0.04 0.37 0.07	0.38 0.53 0.27	0.39 0.57 0.29	0.75 0.75 0.60			
		ΔT					0.19 0.75 0.19	0.03 0.19 0.07	0.04 0.13 0.11
		R	0.15	0.46	0.36	0.76			
19	Gressoney-Saint-Jean	T	0.81 0.76 0.83	0.53 0.49 0.61	0.74 0.73 0.74	<0.09 <0.09 <0.09			

Nat. Hazards Earth Syst. Sci. Discuss., doi:10.5194/nhess-2016-100, 2016
Manuscript under review for journal Nat. Hazards Earth Syst. Sci.
Published: 4 April 2016
© Author(s) 2016. CC-BY 3.0 License.

Natural Hazards and Earth System Sciences
Discussions

		ΔT					0.77 0.73 0.76 0.76 0.80 0.77 0.63 0.74 0.69
		R	/	0.99	0.92	0.51	
	Eastern Italian Alps						
20	Latemar	*T*	0.83 0.76 0.59	0.64 0.78 0.54	<0.06 0.16 <0.04	0.12 0.48 0.06	
		ΔT					0.83 0.66 0.68 0.80 0.61 0.78 0.84 0.74 0.64
		R	0.13	0.45	0.82	0.61	
21	San Vito di Cadore	*T*	0.09 <0.05 0.09	<0.05 <0.05 <0.05	<0.05 <0.05 <0.05	0.46 0.48 0.37	
		ΔT					0.29 0.57 0.13 0.58 0.44 0.50 0.77 0.78 0.86
		R	0.50	0.35	0.51	0.30	
22	Colcuc	*T*	0.83 0.67 >0.95	0.43 0.42 0.30	0.42 0.31 0.52	0.24 0.16 0.28	
		ΔT					0.88 0.87 0.89 0.79 0.52 0.94 0.97 0.96 0.94
		R	0.15	0.22	0.45	0.20	
23	Ivigna	*T*	NA 0.27 <0.03	NA 0.78 0.20	NA 0.50 0.28	NA 0.37 0.38	
		ΔT					NA 0.87 0.04 NA 0.16 0.01 NA 0.14 0.09
		R	/	0.24	0.2	0.23	
24	Torre Trephor	*T*	0.21 0.33 0.46	0.77 0.86 0.67	0.17 0.29 0.15	0.09 0.13 0.11	
		ΔT					0.04 0.08 0.21 0.02 0.02 0.02 0.15 0.11 0.33
		R	0.20	0.63	0.28	<0.05	
25	Cima Dodici I	*T*	0.42 0.41 0.58	0.45 0.46 0.46	0.31 0.34 0.20	<0.05 <0.05 <0.05	
		ΔT					0.47 0.34 0.81 0.19 0.20 0.16 0.80 0.78 0.70
		R	0.83	0.36	0.38	<0.05	
26	Forcella dei Ciampei	*T*	NA 0.41 0.84	NA 0.69 0.61	NA 0.65 0.26	NA 0.44 0.15	
		ΔT					NA 0.18 0.98 NA 0.21 0.24 NA 0.60 0.78
		R	/	0.21	0.17	0.33	
27	Monte Pelmo	*T*	0.82 0.71 0.80	0.57 0.49 0.72	0.78 0.67 0.84	0.27 0.20 0.19	
		ΔT					0.72 0.67 0.40 0.78 0.80 0.58 0.76 0.84 0.51
		R	/	0.56	0.14	0.17	
28	Thurwieser	*T*	NA 0.88 >0.91	NA 0.52 0.62	NA 0.77 0.45	NA 0.51 0.41	
		ΔT					NA 0.95 0.97 NA 0.89 0.90 NA 0.78 0.72
		R	/	0.12	0.2	0.23	
29	Monte Castelin	*T*	0.87 0.53 0.74	0.63 0.55 0.62	0.61 0.56 0.42	0.51 0.43 0.45	
		ΔT					0.58 0.25 0.70 0.78 0.40 0.86 0.61 0.63 0.35
		R	/	0.67	0.37	0.15	
30	Tofana di Rozes	*T*	0.27 0.53 0.12	0.01 0.14 0.09	0.21 0.18 0.13	0.47 0.36 0.40	
		ΔT					0.98 0.98 0.80 0.81 0.87 0.60 0.55 0.68 0.38
		R	/	0.69	0.28	0.31	
31	Monte Pelf	*T*	0.82 0.84 0.66	0.81 0.75 0.82	0.71 0.55 0.69	0.22 0.14 0.15	
		ΔT					0.36 0.32 0.36 0.51 0.51 0.51 0.52 0.62 0.52
		R	0.17	0.06	0.37	0.08	
32	Cima Dodici II	*T*	>0.95 >0.95 0.93	0.86 0.91 0.81	0.91 0.85 0.93	0.58 0.47 0.43	
		ΔT					0.82 0.65 0.82 0.91 0.74 0.92 0.79 0.67 0.77
		R	/	/	0.13	<0.05	
33	Cima Una	*T*	0.50 0.68 0.45	0.53 0.73 0.44	0.54 0.70 0.41	0.31 0.40 0.17	
		ΔT					0.89 0.72 0.87 0.66 0.63 0.54 0.35 0.71 0.22
		R	/	0.26	0.40	0.56	
34	Cima Canali	*T*	0.49 0.45 0.57	0.28 0.26 0.13	0.83 0.81 0.72	0.75 0.78 0.80	
		ΔT					0.93 0.66 0.95 0.91 0.70 0.92 0.52 0.46 0.46
		R	0.05	0.96	0.74	0.92	
35	Cima Undici	*T*	>0.95 0.89 0.93	0.89 0.86 0.81	0.55 0.47 0.64	0.58 0.49 0.82	
		ΔT					0.53 0.36 0.83 0.76 0.55 0.80 0.85 0.70 0.88
		R	/	0.15	0.52	0.74	
36	Plattkofel	*T*	NA 0.42 0.54	NA 0.08 0.28	NA <0.05 <0.05	NA 0.27 0.47	
		ΔT					NA 0.93 0.44 NA 0.96 0.90 NA 0.91 0.65
		R	0.06	0.98	0.97	0.61	
37	Euringer	*T*	NA 0.57 0.16	NA 0.49 0.40	NA 0.44 0.16	NA 0.64 0.61	
		ΔT					NA 0.74 0.62 NA 0.33 0.21 NA 0.55 0.08
		R	/	0.77	0.69	0.54	
38	Sass Maor	*T*	0.36 0.37 0.55	0.23 0.09 0.18	0.19 0.81 0.21	0.89 0.84 0.73	
		ΔT					0.94 0.98 0.94 0.75 0.91 0.75 0.20 0.31 0.20
		R	/	/	0.10	0.11	
39	Sorapiss	*T*	0.44 0.20 0.53	0.83 0.73 0.90	0.70 0.61 0.73	0.83 0.83 0.83	
		ΔT					0.17 0.13 0.26 0.16 0.13 0.20 0.04 0.03 0.11
		R	0.51	0.59	0.29	0.34	
40	Monte Civetta	*T*	0.55 0.68 0.63	0.90 0.83 0.91	>0.95 0.89 >0.95	0.91 0.69 >0.95	
		ΔT					0.57 0.31 0.57 0.15 0.32 0.15 0.51 0.50 0.51
		R	/	0.66	0.59	0.40	
41	Antelao	*T*	0.31 0.40 0.30	0.60 0.63 0.60	0.76 0.75 0.85	0.69 0.52 0.82	
		ΔT					0.50 0.24 0.50 0.13 0.08 0.13 0.05 0.06 0.05
		R	0.78	0.80	0.76	0.70	

1

Nat. Hazards Earth Syst. Sci. Discuss., doi:10.5194/nhess-2016-100, 2016
Manuscript under review for journal Nat. Hazards Earth Syst. Sci.
Published: 4 April 2016
© Author(s) 2016. CC-BY 3.0 License.

Natural Hazards and Earth System Sciences
Discussions
Open Access
EGU

Figures

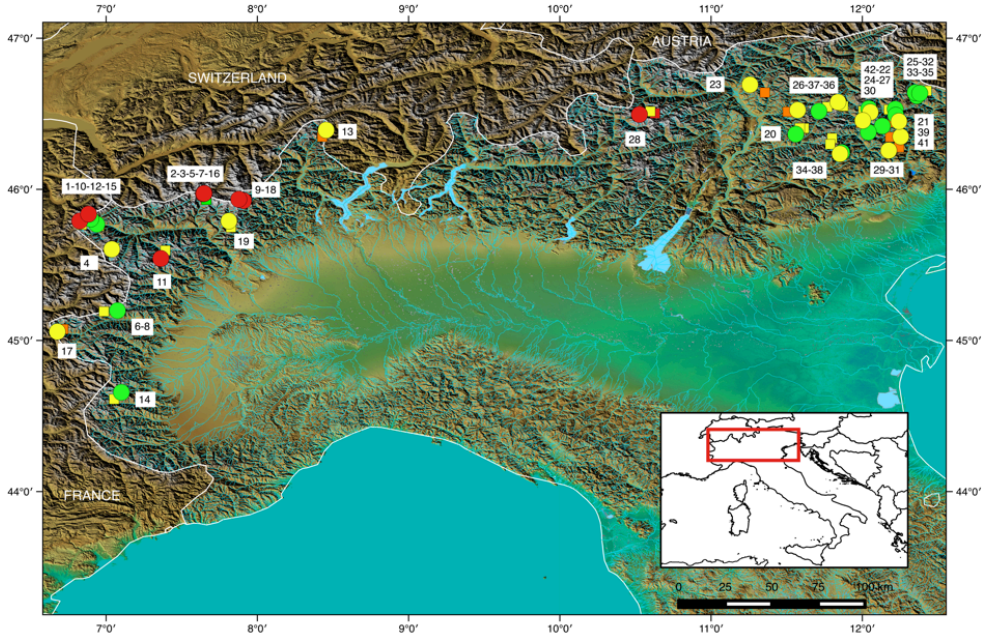

Figure 1. Map showing 41 events included in the inventory (dots) and of the 27 meteorological stations used in the study (squares). Events and meteorological stations are coloured differently according to elevation. Yellow dots/squares represent events/meteorological stations at low elevation (1500-2400 m a.s.l); green dots/squares represent events/meteorological stations at medium elevation (2400-3300 m a.s.l); red dots/squares represent events/meteorological stations at high elevation (3300-4200 m a.s.l); meteorological stations located below 1500 m a.s.l. are in orange. Events are numbered according to Table 1.

Nat. Hazards Earth Syst. Sci. Discuss., doi:10.5194/nhess-2016-100, 2016
Manuscript under review for journal Nat. Hazards Earth Syst. Sci.
Published: 4 April 2016
© Author(s) 2016. CC-BY 3.0 License.

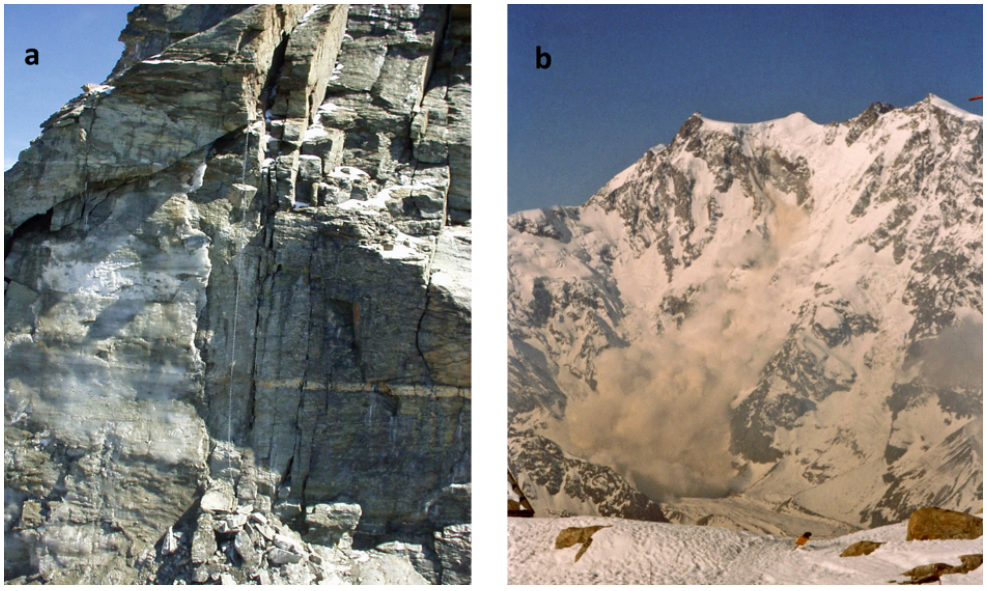

Figure 2. Selected examples of rockfall events. (a) Detachment area of the Matterhorn II rockfall (18 August 2003), with the ice lens (on the left) exposed by the collapse of the rock mass; photo source: L. Trucco. (b) Belvedere rock-avalanche (21 April 2007). The red circle indicates the detachment zone; photo source: F. Bettoli.

Nat. Hazards Earth Syst. Sci. Discuss., doi:10.5194/nhess-2016-100, 2016
Manuscript under review for journal Nat. Hazards Earth Syst. Sci.
Published: 4 April 2016
© Author(s) 2016. CC-BY 3.0 License.

Natural Hazards and Earth System Sciences
Discussions
Open Access
EGU

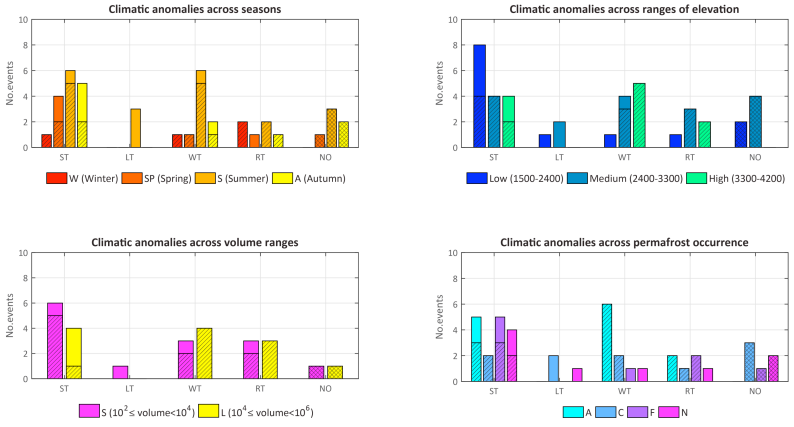

Figure 3. Distribution of rockfalls according to the type of climate anomaly, and considering: (a) the season of occurrence: W (winter), SP (spring), S (summer), A (autumn); (b) the elevation: Low (1500-2400 m); Medium (2400-3300 m); High (3300-4200 m); (c) rockfall volume: small-volume events (S, $10^2 \leqslant$volume$<10^4$ m^3), large-volume events (L, $10^4 \leqslant$volume$<10^6$ m^3); d) expected permafrost occurrence in the detachment zone: A (permafrost in nearly all conditions), C (mostly in cold conditions), F (only in very favourable conditions), N (no permafrost). Climate anomaly groups: ST: short-term temperature anomaly; LT: long-term temperature anomaly; WT: widespread temperature anomaly; R: precipitation anomaly (at the weekly range or longer) without or in association to temperature anomalies; NO: no anomaly. Warm T anomalies are highlighted with a strikethrough overlay.

Nat. Hazards Earth Syst. Sci. Discuss., doi:10.5194/nhess-2016-100, 2016
Manuscript under review for journal Nat. Hazards Earth Syst. Sci.
Published: 4 April 2016
© Author(s) 2016. CC-BY 3.0 License.

Natural Hazards and Earth System Sciences
Discussions

Appendix A

Table A1. Synthetic characterization of case studies and possible processes leading to slope failure. Number (No.) and location of case studies are the same as in Table 1. Climate anomaly: type of anomaly associated to rockfall occurrence: ST: short-term temperature anomaly; LT: long-term temperature anomaly; WT: widespread temperature anomaly; RT: precipitation anomaly -at the weekly range or longer- without or in association to temperature anomalies; NO: no anomaly; positive temperature anomaly ($P(V) \geqslant 1-\alpha/2$) are indicated as + while negative temperature anomaly ($P(V) \leqslant \alpha/2$) are indicated as -; the coexistence of both anomalies is indicated as ±. Season: season of occurrence of rockfalls: W (winter), SP (spring), S (summer), A (autumn). Elevation: Range of elevation z of rockfall niche (m a.s.l.): L ($1500 \leqslant z < 2400$); M ($2400 \leqslant z < 3300$); H ($3300 \leqslant z \leqslant 4200$). Volume: volume of detached rock (m^3): small-volume (S, $10^2 \leqslant$ volume $< 10^4$) and large-volume (L, $10^4 \leqslant$ volume $< 10^6$) events. Permafrost: expected permafrost occurrence in the detachment zone: A (permafrost in nearly all conditions), C (mostly in cold conditions), F (only in very favourable conditions), N (no permafrost).

No.	Location	Climate anomaly	Season	Elevation	Volume	Permafrost	Hypothesized processes leading to slope failure
1	Brenva	RT	W	H	L	A	Exceptional precipitation in the months preceding the event may have caused the onset of high water pressure in the rock slope. Frost penetration inside the slope during the winter may have been responsible for further groundwater pressure increase, leading finally to failure.
2	Matterhorn I	WT+	S	H	S	A	Permafrost thaw
3	Matterhorn II	WT+	S	H	S	A	Permafrost thaw
4	Mont Pelà	LT-	S	L	S	N	Rain on snow. The negative LT anomaly at the quarterly scale may have preserved the snowpack until mid-summer. The addition of snow melting to rain may have caused the slope failure.
5	Matterhorn III	ST+	S	H	-	A	Melting of winter snowpack due to a sudden temperature rise in the days (1-6) preceding the failure.
6	Rocciamelone I	ST+	S	M	-	A	No proposed explanation
7	Matterhorn IV	WT+	S	H	-	A	Permafrost thaw
8	Rocciamelone II	WT+	W	M	L	A	No proposed explanation
9	Belvedere	WT+	SP	H	L	A	According to Huggel et al. (2010), even if air temperature at the niche must have been well below 0°C in the days preceding the rockfall, the intense solar radiation might have caused snow and ice melting. Besides the triggering factor, the predisposing conditions for this failure relate to the rapid evolution undergone by the eastern face of the Monte Rosa massif since the late 90s: in particular, this rockfall occurred two years after a huge icefall that detached just below this rockfall niche (Tamburini et al., 2013).
10	Tré-la-Tête	RT+	S	H	L	A	Exceptional precipitation at the quarterly scale may have caused the onset of high water pressure in the rock slope. The sudden increase of Tmax in the days (1-3) preceding the event may have caused the melting of an early snowfall, triggering slope failure.
11	Punta Patri Nord	ST-	S	H	L	A	Freezing of water springs along the slope, blocking the

Nat. Hazards Earth Syst. Sci. Discuss., doi:10.5194/nhess-2016-100, 2016
Manuscript under review for journal Nat. Hazards Earth Syst. Sci.
Published: 4 April 2016
© Author(s) 2016. CC-BY 3.0 License.

Natural Hazards and Earth System Sciences Discussions

							seepage of water from the permafrost thaw through the rock mass: the build-up of high water pressure may have caused the collapse of the rock mass.
12	Crammont	RT+	W	M	L	F	No proposed explanation about the event trigger. Deline et al. (2013) relate the occurrence of this rockfall to permafrost degradation, based on the presence of seepage water in the scar after the collapse, in spite of negative air temperatures.
13	Val Formazza	ST-	SP	L	L	N	Freezing of water springs along the slope and consequent blockage of snowmelt water seepage through the rock mass: the high water pressure caused by the blockage of the water flow may have caused the collapse of the rock mass.
14	Monviso	NO	S	M	S	C	No detected anomaly
15	Mont Rouge Peutery	NO	S	M	-	F	No detected anomaly
16	Matterhorn V	WT+	S	H	-	A	Permafrost thaw
17	Melezet	ST+	SP	L	S	N	Accelerated snow melt due to sudden temperature increase
18	Punta Tre Amici	ST-	A	H	L	A	Freezing of water springs along the slope, blocking the seepage of water from the permafrost thaw through the rock mass: the build-up of high water pressure may have caused the collapse of the rock mass.
19	Gressoney-Saint-Jean	RT-	SP	L	S	N	Snow melt of an exceptionally deep snow pack. The amount of water released by snowmelt may have been particularly relevant because of the combination of a cold temperature anomaly at the quarterly scale with extraordinary precipitations in the month before the event, resulting in a deep snowpack.
20	Latemar	LT-	S	M	-	C	Snow melt of an exceptionally deep snow pack. The amount of water released by snowmelt may have been particularly relevant because of the combination of a cold temperature anomaly at the quarterly scale with extraordinary precipitations in the month before the event, resulting in a deep snowpack.
21	San Vito di Cadore	WT-	A	M	S	F	Freezing of water springs along the slope and consequent blockage of water seepage through the rock mass: the high water pressure caused by the blockage of the water flow may have caused the collapse of the rock mass.
22	Colcuc	ST+	SP	L	S	N	Accelerated snow melt due to sudden temperature increase
23	Ivigna	ST-	SP	L	-	N	Freezing of water springs along the slope and consequent blockage of snowmelt water seepage through the rock mass: the high water pressure caused by the blockage of the water flow may have caused the collapse of the rock mass.
24	Torre Trephor	WT-	SP	L	-	N	Freezing of water springs along the slope and consequent blockage of snowmelt water seepage through the rock mass: the high water pressure caused by the blockage of the water flow may have caused the collapse of the rock mass.
25	Cima Dodici I	LT-	S	M	-	C	Rain on snow. The negative LT anomaly at the quarterly scale may have preserved the snowpack until the date of the event. The addition of snow melting to rain may have

Nat. Hazards Earth Syst. Sci. Discuss., doi:10.5194/nhess-2016-100, 2016
Manuscript under review for journal Nat. Hazards Earth Syst. Sci.
Published: 4 April 2016
© Author(s) 2016. CC-BY 3.0 License.

Natural Hazards and Earth System Sciences Discussions

							caused the slope to fail.
26	Forcella dei Ciampei	ST+	S	L	S	N	Accelerated snowmelt due to sudden temperature increase the day of the event.
27	Monte Pelmo	NO	S	M	-	C	No detected anomaly
28	Thurwieser	ST+	S	H	L	A	Accelerated permafrost thaw due to sudden temperature increase in the days (1-3) preceding the event.
29	Monte Castelin	NO	A	L	-	N	No detected anomaly
30	Tofana di Rozzes	ST±	S	M	-	F	Rapid melting of an early snowfall. Temperature suddenly raised in the day of the event, following extraordinarily low temperatures and heavy precipitation in the week before the event.
31	Monte Pelf	NO	SP	L	-	N	No detected anomaly
32	Cima Dodici II	WT+	S	M	L	C	Rapid snowmelt caused by extraordinarily high temperatures in the month and in the days preceding the event.
33	Cima Una	NO	A	M	L	C	No detected anomaly
34	Cima Canali	RT+	S	M	S	F	Heavy precipitations in the week and in the months preceding the event. No proposed explanation for the trigger.
35	Cima Undici	ST+	S	M	S	C	No proposed explanation
36	Plattkofel	RT±	S	M	S	C	Rapid melting of an early snowfall. Temperature suddenly raised the day of the event, following extraordinarily low temperatures and heavy precipitation in the month before the event.
37	Euringer	ST-	S	L	S	F	Freezing of water springs along the slope and consequent blockage of snowmelt water seepage through the rock mass: the high water pressure caused by the blockage of the water flow may have caused the collapse of the rock mass.
38	Sass Maor	ST±	W	L	-	F	No proposed explanation
39	Sorapiss	ST±	A	M	S	C	Freezing of water springs along the slope and consequent blockage of water seepage through the rock mass: the high water pressure caused by the blocking of the water flow may have caused the collapse of the rock mass.
40	Monte Civetta	WT+	A	M	L	C	Warm temperatures allowed precipitations to fall as rain rather than as snow in the week and month before the event.
41	Antelao	ST-	A	L	-	F	Freezing of water springs along the slope and consequent blockage of water seepage through the rock mass: the high water pressure caused by the blocking of the water flow may have caused the collapse of the rock mass.

1
2
3